RSC Advances

ROYAL SOCIETY OF CHEMISTRY

www.rsc.org/advances

RSC Advances

RSCPublishing

ARTICLE

Cite this: DOI: 10.1039/x0xx00000x

Received 00th June 2014,
Accepted 00th June 2014

DOI: 10.1039/x0xx00000x

www.rsc.org/

Monodisperse, Nanoporous Ceria Microspheres Embedded with Pt Nanoparticles: General Facile Synthesis and Catalytic Application

Lin Zhou [a], Xiaoxiao Li [b], Yong Wang [a], Mei Hong *[a], Yongye Liang *[b], and Jing Zhao *[a, c]

A monodisperse Pt/ceria hybrid with controlled nanoporous structure was fabricated with the aid of poly (glycidyl methacrylate-co-ethylene glycol dimethacrylate) microspheres as hard template. Functional groups on the polymer microspheres interacted with Pt species and then cerium precursors were impregnated into the microsphere pores through a sol-gel method. Porous ceria microspheres embedded with uniform and fine Pt nanoparticles formed after removing the polymer templates by calcination. Hierarchical Pt/ceria hybrid could afford superior catalytic activity, excellent stability and easily recyclable. For example, highly efficient catalytic reduction of 4-nitrophenol (4-NP) with sodium borohydride was accomplished. The facile and general synthetic method could extend to other novel metal/oxide hybrid combinations.

Introduction

Catalytic properties of a supported metal system are found to be closely related to the type and morphology of supports involved.[1] As supports, metal oxides could efficiently prevent the dispersed metal nanoparticles from agglomeration and deactivation[2]. Ceria (CeO_2) has been applied as support to construct catalysts for a wide variety of reactions, such as CO oxidation,[3] hydrogenation[4] and water-gas shift[5]. The advantages of ceria in catalysis could be attributed to its intrinsic features, such as abundant oxygen vacancy defects, peerless oxygen storing/releasing capabilities, as well as easy shuttle between the III and IV oxidation states.[6] In particular, noble metal/ceria-based catalysts are long known to exhibit strong metal–support interaction effects,[7] in which rapid activated oxygen and/or electron transfer between metal and support could be involved.[8] Such metal-support interaction was reported to increase the catalytic activity and selectivity of Pt.[9] Thus, design of heterogeneous catalysts composed of ceria with Pt nanoparticles is of fundamental importance.

To achieve high catalytic activity, the noble metal is usually prepared as nanoparticles while the metal supports are in the form of porous structure. Easy preparation methods and recycled application are highly desirable. Noble metal/oxide catalysts are usually prepared through template-free methods, lacking precise control over the structure and morphology of the catalysts. Several novel methods have recently been reported to prepare noble metal/oxide catalysts with secondary nanostructures. Notably, Wang and co-workers reported a general method for the fabrication of mesoporous oxides loaded with noble metal nanoparticles by aerosol spraying and solvent-evaporation-induced assembly.[10] Zhang *et al.* designed an ingenious route to uniform pomegranate-like Pt@ceria nanospheres by redox reaction in Argon.[11] Yet it remains challenging to prepare well-controlled and uniform catalyst structures. Hard template methods could offer easy access to structures with well-defined pore architecture and high surface area, which are required for high catalytic performance.[12] For example, silica templates, such as SBA-15, SBA-16, MCM-48 and KIT-6 have been used for the synthesis of ceria nanomaterials.[13] However, several limitations of these approaches prevent them from wider applications. Specifically:

(1) an additional step is required to dissolve the silica template after the formation of ceria;

(2) hazardous chemicals are sometimes required, such as HF;

(3) formation of diverse structural defects in ceria due to the oxygen linkage between silica and ceria after removing the silica template.

On the other hand, organic templates have also been used for controlled synthesis of metal oxides and could be simply removed in the calcination process.[14] Especially interesting are polymer templates with relatively robust structures, providing great opportunities to prepare complex noble metal/metal hybrid structures with required properties.[15] Herein we present a feasible template-based approach for the fabrication of uniform, nanoporous Pt/CeO_2 hybrid microspheres (**Figure 1**).

The advantages of polymer microsphere templates include well-controlled size and porosity and easily functionalized surface.[16] By removing the organic polymer templates, a hierarchical structure of fine Pt nanoparticles embedded on porous ceria microspheres was formed. These hybrid structures showed superior catalytic activities in the reduction of 4-nitrophenol (4-NP) to 4-aminophnol (4-AP)[17] compared to the Pt/ceria composite prepared without a template. The microsized catalyst was easily recycled with high recovery ratios and the activity was sustained after 5 cycles. This new approach to construct metal nanoparticles embedded in porous metal oxide microspheres could pave a new way to synthesize efficient catalysts with good stability and easy recyclability.

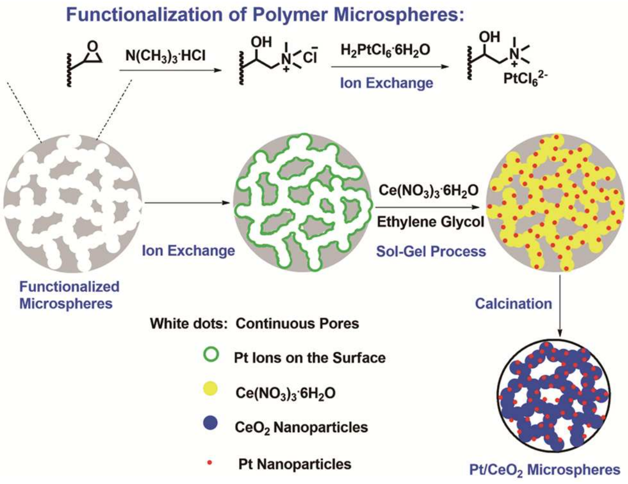

Scheme 1 Synthetic scheme of porous Pt/CeO_2 hybrid microspheres.

Results and discussion

The preparation strategy of Pt/CeO_2 microspheres was shown in **Figure 1**. Functionalized porous microspheres of poly (glycidyl methacrylate-co-ethylene glycol dimethacrylate), poly (GMA-co-EGDMA), were used as the sacrificed templates. The morphology and pore architecture of the obtained ceria microspheres could be simply adjusted by varying the polymer microspheres applied. Here, polymer microspheres with a diameter of 7.5 µm were chosen to construct the hybrid structure. Such size could offer easy recycle of ceria hybrid materials in catalysis application. SEM images of the polymer microsphere template were shown in **Figure S1**, suggesting porous structure and uniform size distribution of the microspheres. Textural properties of the polymer microspheres were shown in **Figure S2**. Surface area of the polymer microspheres was 114 m^2/g, and the pore volume was 0.8 cm^3/g, whose porous structure was suitable for adsorbance of metal ions and cerium gels. The surface of the monodisperse polymer microspheres was initially functionalized with quaternary ammonium group via ring-opening reaction of epoxide groups of GMA with trimethylamine hydrochloride, and polymer microspheres terminated with large amount of quaternary ammonium groups were obtained. FT-IR spectra of the the polymer microsphere before and after reaction (**Figure S3**) confirmed the successful functionalization of the hard template. Then $PtCl_6^{2-}$ was adsorbed onto the surface of the quaternary ammonium group-terminated microspheres through ion exchange with Cl^-. Cerium (III) nitrate was impregnated into the microspheres, followed by the addition of ethylene glycol acting as a reducing agent. The mixture was then heated at 60 °C in the drying oven, forming the ceria gel and generating Pt nanoparticles.[18] It was observed that cerium gel was fully adsorbed into the pores of polymer microspheres during this process, and no nucleation of the CeO_2 nanoparticles outside the microspheres was detected (**Figure S4**). The Pt/Polymer-ceria hybrid was then calcined in a muffle furnace at 600 °C for 12 h. During the calcination process, the ceria nanoparticles formed gradually and yielded the microspheres loaded with Pt NPs. When the temperature reached 500 °C, the polymer hard template was removed and the residual ethylene glycol was burned off.[16]

The scanning electron microscopy (SEM) images (**Figure 2a, 2b**) indicated that the resulting Pt/CeO_2 microspheres were uniform and monodisperse, with morphologies similar to their parent polymer microspheres. Particle size of the polymer microspheres changed from 7.5 µm to 4.0 µm after calcination when ceria microspheres formed (**Figure S5**), which might due to shrinkage of the skeleton and increase in density of ceria during the thermal treatment to remove polymeric template. The transmission electron microscopy (TEM) image in **Figure 2c** clearly revealed the porous structure of these microspheres. Different diameters of CeO_2 thin slices in **Figure 2c** were developed during the process of preparing TEM samples on a ion slicer as slices were cut through different parts of every single Pt/CeO_2 microsphere. We observed dark spots distributing over the whole microspheres, which could correspond to crystalline CeO_2 and platinum nanoparticles (**Figure 2d**). The major (111) crystalline planes with 0.311 nm distance of CeO_2 were dominantly observed, and the particle size of these crystalline ceria nanoparticles was around 5-10 nm (**Figure 2d** bottom inset). We also observed a few fine Pt nanoparticles (circles in **Figure 2d**) with size of 2-5 nm in the high resolution TEM (HRTEM) image, and the lattice fringes corresponded to (111) crystalline plane of Pt as could be seen in the enlarged image in **Figure 2d** (right middle inset) and. **Figure S6.** The dark field scanning transmission electron microscopy image (STEM-DF) of the Pt/CeO_2 sample was shown in **Figure 3a**, further revealing the hierarchic structures of the hybrid, with small dots with size of around 1-2 nm embedded in the larger nanoparticles with size of 5-10 nm.

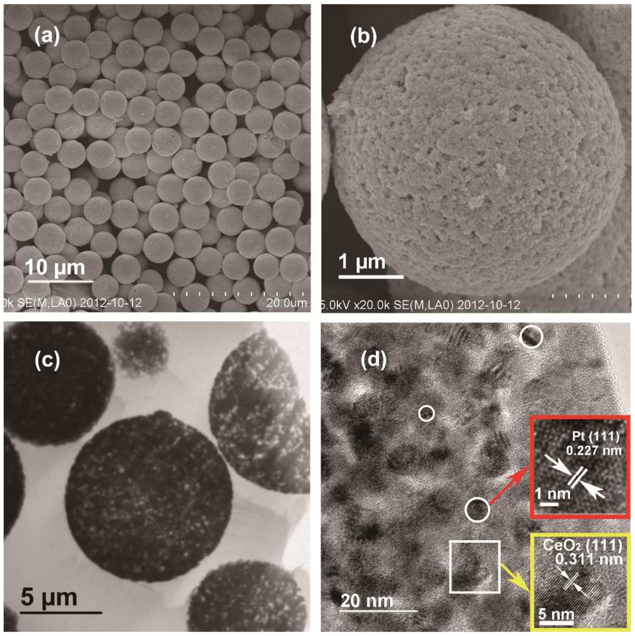

Scheme 2 SEM images and TEM images of Pt/CeO_2 microspheres: (a, b) SEM images of Pt/CeO_2 microspheres; (c) low resolution TEM image and (d) high resolution TEM image of Pt/CeO_2 microspheres (The bottom inset showed the enlarged image of a CeO_2 nanoparticle while the top inset showed the enlarged image of a Pt nanoparticle).

The element distribution obtained from the energy-dispersive X-ray spectroscopy (EDS)-mapping indicated the uniform distribution of the Pt, Ce, O elements in the whole microsphere hybrid (**Figure**

3b-d). The distribution of the small dots in STEM-DF correlated well with the Pt mapping, suggesting the small dots could be Pt nanoparticles. It is consistent with the HRTEM image that the size of the Pt nanoparticles was very small.

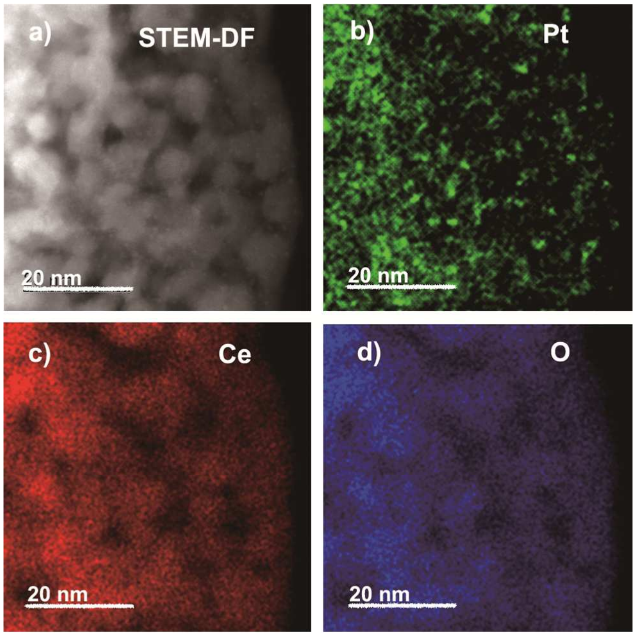

Scheme 3 a) STEM-DF images of a detailed view on an individual Pt/CeO_2 microsphere and the corresponding elemental mappings of b) Pt, c) Ce and d) O.

The XRD of Pt/CeO_2 microspheres showed sharp diffraction peaks corresponding to the face-centered cubic phase of ceria (JCPDS No. 34-0394), indicating good crystallinity (**Figure S7).** No obvious peaks of Pt nanoparticles were observed, partly due to its ultra-fine particle size. The N_2 adsorption-desorption isotherm of Pt/CeO_2 microspheres had a hysteresis loop in the range of relative pressures P/P_0 = 0.60-0.99, indicating the mesoporous structures of the ceria microspheres (**Figure S8a**). The BJH pore size distribution of Pt/CeO_2 microspheres (**Figure S8b**) exhibited a distribution between 1 and 50 nm. BET surface area of the microspheres was 38 m^2/g, with an average pore diameter of 14 nm. The loading of Pt in Pt/CeO_2 microspheres was determined by atomic absorption spectroscopy with optical emission spectrometer, which was 7.7 wt%. Pt/CeO_2 composite was also prepared via similar but template-free method as a control to the Pt/CeO_2 microspheres. SEM images of the Pt/CeO_2 composite revealed its lack of structural regularity (**Figure S9**).

Catalytic Study

The catalytic activities of the Pt/CeO_2 microspheres were evaluated by the catalytic reduction reaction of 4-NP to 4-AP, as shown in **Figure 4a**. The absorption peak at 400 nm, corresponding to the formation of 4-nitrophenolate ion in alkaline conditions,[17] remained unchanged in the absence of the catalysts and gradually decreased in intensity after the addition of a very small amount of the Pt/CeO_2 microsphere. Concomitant increase of a new peak at 300 nm was observed, corresponding to the formation of 4-AP, the reduction product of 4-NP. **Figure 4b** (right top inset) illustrated the absorption change of the above catalytic reduction process. The reaction rates were assumed to follow pseudo-first-order kinetics with respect to the reactants with a large excess of $NaBH_4$ relative to 4-NP. Linear relationship between ln[C(t)/C(0)] and reaction time was obtained, where *C*(t) and *C*(0) represented the concentration of 4-NP at time t and at the beginning of the reaction. The rate constants (k) were determined from the slopes and represented different reaction activities of the catalysts. Plot of ln[C(t)/C(0)] against the reaction time of Pt/CeO_2 microspheres was shown in **Figure 4b** and the rate constant was calculated to be 0.287 min^{-1}.

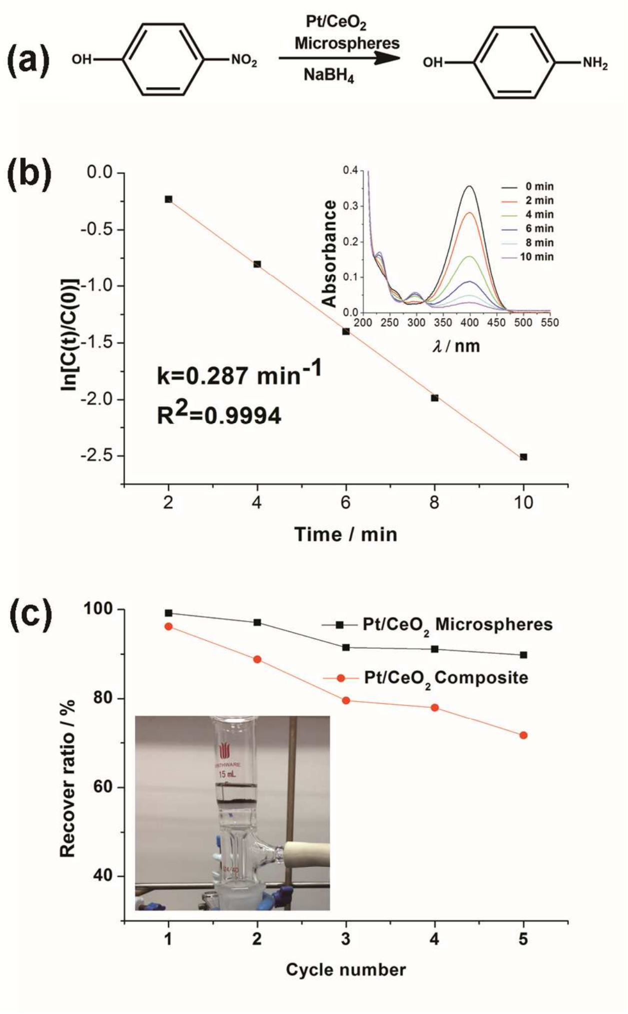

Scheme 4 (a) Reaction equation of catalytic reduction of 4-NP to 4-AP; (b) Plot of ln[C(t)/C(0)] against the reaction time by Pt/CeO_2 hybrid catalyst; and (c) Recovery ratio of Pt/CeO_2 microspheres and Pt/CeO_2 composite (5 cycles).

With the presence of only CeO_2 microspheres or bare Pt nanoparticles, the model system showed little absorbance change after the addition of $NaBH_4$, suggesting the low catalytic activity of the single component and the importance of the Pt/CeO_2 hybrid structure for catalysis (**Figure S10**). It should be noted that both the porous CeO_2 microspheres and Pt particles showed little absorption of the 4-NP during the measurements. It confirmed that the absorbance change in Pt/CeO_2 system was caused by the reaction of 4-NP, instead of absorption in the porous microspheres. A control test was conducted with Pt/CeO_2 composite at the same reaction condition (**Figure S11**). The Pseudo-first-order rate constant of

Pt/CeO_2 composite was 0.069 min^{-1}, which was much smaller than that of Pt/CeO_2 microsphere catalyst (0.287 min^{-1}). The reaction time (90% of 4-NP consumed) of Pt/CeO_2 composite catalysts (40 min) was about 4 times as much as that of Pt/CeO_2 microspheres (11 min) under the same reaction condition. The hierarchical porous CeO_2 microsphere support probably accounted for the higher catalytic activity of the Pt/CeO_2 microspheres compared to the structure-irregular composite materials. Pt nanoparticles were uniformly dispersed on the metal oxide supports without obvious aggregation, which helped improve catalytic activities of the Pt/CeO_2 hybrid catalyst for this diffusion-controlled reaction.

Recycling test was carried out to evaluate the reusability of Pt/CeO_2 microspheres after liquid phase catalytic reduction of 4-NP to 4-AP reaction cycles. Reaction time of each cycle was defined as the time (min) when 90% of 4-NP was consumed, which was shown in **Figure S12**. The catalytic efficiencies of the Pt/CeO_2 microspheres remained relatively constant after 5 successive cycles. In the second recycle, activity dropped a little and reaction time changed from 11 min to 14 min. Then the reaction time was relatively well maintained, between 14 min and 16 min in the following four cycles. Instability of $NaBH_4$ might have effects on the results of the recyclability of Pt/CeO_2 catalysts and a 10% weight loss of catalysts during recovery process would also resulted in the decrease of catalytic activity after 5 cycles.[11] A study of recovery ratio was also performed in the model reaction of 4-NP to 4-AP. The results shown in **Figure 4c** demonstrated that Pt/CeO_2 microspheres were easily recovered through centrifugation at 2000 rpm and the recovery ratio remained above 90% after 5 cycles, while the recovery ratio of Pt/CeO_2 composite dropped to 72%. Actually, Pt/CeO_2 microspheres could be recycled through sand core funnel, which was shown in **Figure 4c inset**. Further, our catalysts could survive after thermal treatment at 700 °C and even higher at 800 °C with no catalytic activity loss in the model system (**Figure S13**). It's believed that the microsized and monodispersed structures of the Pt/CeO_2 hybrid improved the cycling ability of the catalyst.

With this general template-mediated method in hand, Au/CeO_2, Pd/CeO_2, Ag/CeO_2 and Cu/CeO_2,microspheres were synthesized through a similar approach to that of Pt/CeO_2 microspheres. For the synthesis of Au and Pd nanoparticles, quaternary ammonium group-terminated polymer microspheres were involved. Au nanoparticles were obtained *in situ* as the quaternary ammonium functional groups on the microspheres could reduce $AuCl_4^-$ during the calcination process. PdO nanoparticles deposited on CeO_2 microspheres were reduced to Pd nanoparticles using hydrazine hydrate as a reducing agent. Ag and Cu nanoparticles were developed from sulfonated microspheres (**Scheme S14**). AgO nanoparticles decomposed under the calcination temperature and Ag nanoparticles formed. Hydrogen reduction was performed to guarantee the formation of Cu nanoparticles after calcination. The SEM images of the various metal NPs/CeO_2 microspheres were shown in **Figure S15**, indicating that all the metal NPs loaded ceria microspheres as-prepared possessed porous structure with uniform size distribution. EDS-mappings of Au/CeO_2 and Pd/CeO_2 microspheres were shown in **Figure S16** and **Figure S17** respectively, indicating the uniform distribution of Au and Pd nanoparticles. Metal loadings of those metal NPs/CeO_2 microspheres were listed in **Table S1**. Other metal oxide support, like ZrO_2, could be synthesized by a similar fabrication method.[19] As such, our approaches could be extended to a wide broad range of noble metal/metal oxide hybrids with nanoporous and monodispersed structures.

Conclusions

In summary, we have presented a simple and general route for the fabrication of metal nanoparticles deposited on uniform and porous ceria microspheres by employing poly (GMA-co-EGDMA) microspheres as hard template. The nanoporous, hierarchical and microsized Pt/CeO_2 hybrid structure exhibited high catalytic activities and good recycling stability, as well as easy recovery. This general synthetic method could furnish uniform and porous metal oxide microspheres embedded with metal nanoparticle, opening door to advanced catalysts in various catalytic applications.

Experimental Section

Chemicals and Materials

The ceria precursor cerium (III) nitrate hexahydrate ($Ce(NO_3)_3\cdot 6H_2O$) was purchased from Beijing Ouhe. Hydrochloroplatinic acid ($H_2PtCl_6\cdot 6H_2O$), chloroauric acid tetrahydrate ($HAuCl_4\cdot 4H_2O$), palladium nitrate dehydrate ($Pd(NO_3)_2\cdot nH_2O$) and trimethylamine hydrochloride ($N(CH_3)_3\cdot 6HCl$) were purchased from Sinopharm Chemical Reagent Co., Ltd. Cupric nitrate ($Cu(NO_3)_2$) was purchased from Tianjin Damao. Silver nitrate ($AgNO_3$), sodium borohydride ($NaBH_4$) and 4-nitrophenol (4-NP) were supplied by Alfa Aesar. Sodium sulfite (Na_2SO_3) was purchased from Tianjin Zhiyuan. Porous polymer microspheres named poly (GMA-co-EGDMA) was supplied by Nano-Micro Technology Company, China. Polyvinyl pyrrolidone (PVP) was purchased from Sigma Aldrich. Water was purified by distillation followed by deionization using ion exchange resins. All chemicals were analytical grade and used without further purification.

Characterization Techniques:

Powder X-ray diffraction (XRD) of Pt nanoparticles/CeO_2 microspheres was recorded using a Rigaku D/Max-2200PC diffractometer in the diffraction angle range $2\theta = 10–80^o$ with Cu Kα radiation at 40 KV, 200 mA. The morphology and size of the microspheres were observed by field emission scanning electron microscope (FESEM) on a Hitach S4800 scanning electron microscope (Japan). The transmission electron microscopy (TEM) was performed on JEOL JEM-2100F field emission source transmission electron microscope operated at 200 kV and TEM-EDS x-ray mapping was conducted by using an IET X-max80 machine (Britain). N_2 adsorption/desorption isotherms, BET (Brunauer-Emmett-Teller) surface area, pore volume, and pore size of the microspheres were measured at liquid nitrogen temperature (-196 ^oC) on a Micromeritics Tristar II 3020 v1.03 analyzer (USA). Prior to the measurement, samples were subjected to vacuum system, and then kept under vacuum at 120 ^oC C for at least 12 h. UV adsorption spectra of the catalytic reduction of 4-NP to 4-AP were measured ranging from 200 nm to 600 nm using a Shimadzu UV-2006 UV-Vis Spectrophotometer (Japan). The particle size distribution was measured using a coulter counter Multisizer 3 (Germany).

Procedures for the Preparation of Monodisperse Porous Ceria Microspheres Embedded with Pt Nanoparticles

40 mL of 0.02 mol/L $PtCl_6^{2-}$ solution was added into the suspension of 5 g of quaternary ammonium group-terminated polymer microspheres dispersed in 200 mL distilled water. After stirring for 6 h at room temperature, the mixture was

filtered through sand core funnel and washed repeatedly with water. Then the microspheres were dried in the oven at 60 ^oC for 6 h. To a suspension of 1 g of those microspheres adsorbed with platinum cations in 3 mL water, 2 g of $Ce(NO_3)_3 \cdot 6H_2O$ in 2 mL water was added into the mixture, and 1 g of ethylene glycol was added as a reducing agent to obtain Pt nanoparticles. The mixed solution was transferred to oven set at 60 ^oC and then heat-treated for 6 h. Finally, the obtained poly (GMA-co-EGDMA)/cerium microspheres with platinum cations or nanoparticales was calcined at 600 ^oC for 12 h.

Catalytic Study

For catalytic reduction of 4-NP, aqueous solution of 4-NP (5 mM, 5 mL) was mixed with fresh aqueous solution of $NaBH_4$ (0.4 M, 25 mL) in a three-necked round-bottom flask, and then 2 mL aqueous dispersion of Pt/CeO_2 microspheres (2.0 mg) was rapidly added with mechanical stirring at room temperature. The UV-visible absorption spectra of the reaction mixture were recorded to monitor the reaction progress. Catalytic activities of the catalysts were estimated by pseudo-first-order rate constants of plot of ln[C(t)/C(0)] against the reaction time.

Recyclability Test

In the recyclability test, 2 mg of the Pt/CeO_2 microspheres (Pt/CeO_2 composite) was dispersed in fresh aqueous solution of $NaBH_4$ (0.4 M, 25 mL), and then aqueous solution of 4-NP (5 mM, 5 mL) was added into the solution with mechanical stirring. The UV-visible absorption value for the peak at 400 nm was measured over the whole reaction every 2 minutes. After the reaction completed, the microspheres were collected through centrifugation at 2000 rpm for 2 min and washed with water and alcohol. The catalysts were dried and reused directly without further treatment for another 4 cycles. Activities were evaluated by reaction time.

Acknowledgements

This work is financially supported by grants from the National Basic Research Program of China (2010CB923303), the National High Technology Research and Development Program of China (2014AA020512). J. Z. thanks the Shenzhen Government (SW201110018, JC201104210113A , KQC201105310016A) for support.1).

Notes and references

[a] Guangdong Key Lab of Nano-Micro Materials Research, School of Chemical Biology and Biotechnology, Peking University Shenzhen Graduate School , Shenzhen, 518055, China. Email: jingzhao@pkusz.edu.cn;

[b] Department of Materials Science & Engineering, South Unversity of Science & Technology of China, Shenzhen, 518055, China. Email: liang.yy@sustc.edu.cn;

[c] State Key Laboratory of Pharmaceutical Biotechnology, Institute of Chemistry and Biomedical Sciences, School of Life Sciences, Nanjing University, Nanjing, 210093, China.

† Footnotes should appear here. These might include comments relevant to but not central to the matter under discussion, limited experimental and spectral data, and crystallographic data.

Electronic Supplementary Information (ESI) available: [details of any supplementary information available should be included here]. See DOI: 10.1039/b000000x/

1 (a) S. J. Tauster, S. C. Fung, R. L. Garten, *J. Am. Chem. Soc.* **1978**, 100, 170-175; (b) G. Dutta, U. V. Waghmare, T. Baidya, M. S. Hegde, *Chem. Mater.* **2007**, 19, 6430-6436.

2 C. Chen, C. Nan, D. Wang, Q. Su, H. Duan, X. Liu, L. Zhang, D. Chu, W. Song, Q. Peng, Y. Li, *Angew. Chem. Int. Ed.* **2011**, 50, 3725-3729.

3 C. Hardacre, R. M. Ormerod, R. M. Lambert, *J. Phys. Chem.* **1994**, 98, 10901-10905.

4 (a) M. Abid, R. Touroude, *Catal. Lett.* **2000**, 69, 139-144; (b) J. Silvestre-Albero, F. Rodríguez-Reinoso, A. Sepúlveda-Escribano, *J. Catal.* **2002**, 210, 127-136.

5 (a) Q. Fu, H. Saltsburg, M. Flytzani-Stephanopoulos, *Science* **2003**, 301, 935-938; (b) D. Tibiletti, A. Goguet, F. C. Meunier, J. P. Breen, R. Burch, *Chem. Commun.* **2004**, 1636-1637.

6 (a) C. T. Campbell, C. H. F. Peden, *Science* **2005**, 309, 713-714; (b) F. Esch, S. Fabris, L. Zhou, T. Montini, C. Africh, P. Fornasiero, G. Comelli, R. Rosei, *Science* **2005**, 309, 752-755.

7 (a) J. A. Farmer, C. T. Campbell, *Science* **2010**, 329, 933-936; (b) S. Bernal, J. Kaspar, A. Trovarelli, *Catal. Today* **1999**, 50, 173-173.

8 (a) G. N. Vayssilov, Y. Lykhach, A. Migani, T. Staudt, G. P. Petrova, N. Tsud, T. Skála, A. Bruix, F. Illas, K. C. Prince, V. r. Matolı´n, K. M. Neyman, J. Libuda, *Nat. Mater.* **2011**, 10, 310-315; (b) A. Caballero, J. P. Holgado, V. M. Gonzalez-delaCruz, S. E. Habas, T. Herranz, M. Salmeron, *Chem. Commun.* **2010**, 46, 1097-1099; (c) S. Bernal, J. J. Calvino, M. A. Cauqui, J. M. Gatica, C. Larese, J. A. Pérez Omil, J. M. Pintado, *Catal. Today* **1999**, 50, 175-206.

9 M. A. Vannice, C. C. Twu, S. H. Moon, *J. Catal.* **1983**, 79, 70-80.

10 Z. Jin, M. Xiao, Z. Bao, P. Wang, J. Wang, *Angew. Chem. Int. Ed.* **2012**, 51, 6406-6410.

11 X. Wang, D. Liu, S. Song, H. Zhang, *J. Am. Chem. Soc.* **2013**, 135, 15864-15872.

12 (a) X. Ji, K. T. Lee, L. F. Nazar, *Nat. Mater.* **2009**, 8, 500-506; (b) P. G. Bruce, B. Scrosati, J. M. Tarascon, *Angew. Chem. Int. Ed.* **2008**, 47, 2930-2946; (c) C. Y. Ma, Z. Mu, J. J. Li, Y. G. Jin, J. Cheng, G. Q. Lu, Z. P. Hao, S. Z. Qiao, *J. Am. Chem. Soc.* **2010**, 132, 2608-2613.

13 (a) F. Kleitz, S. H. Choi, R. Ryoo, *Chem. Commun.* **2003**, 2136-2137; (b) B. Tian, X. Liu, H. Yang, S. Xie, C. Yu, B. Tu, D. Zhao, *Adv. Mater.* **2003**, 15, 1370-1374; (c) W. Yue, W. Zhou, J. *Mater. Chem.* **2007**, 17, 4947-4952; (d) F. Ying, S. Wang, C.-T. Au, S.-Y. Lai, *Micropor. Mesopor. Mater.* **2011**, 142, 308-315.

14 (a) M. Agrawal, S. Gupta, A. Pich, N. E. Zafeiropoulos, M. Stamm, *Chem. Mater.* **2009**, 21, 5343-5348; (b) M. Sanlés-Sobrido, M. Pérez-Lorenzo, B. Rodríguez-González, V. Salgueiriño, M. A. Correa-Duarte, *Angew. Chem. Int. Ed.* **2012**, 51, 3877-3882. (c) Y. Chen, J. Lu, J. *Porous Mater.* **2012**, 19, 289-294.

15 K. Yoon, Y. Yang, P. Lu, D. Wan, H. C. Peng, K. Stamm Masias, P. T. Fanson, C. T. Campbell, Y. Xia, *Angew. Chem. Int. Ed.* **2012**, 124, 9681-9684.

16 (a) J. He, C. Yang, X. Xiong, B. Jiang, *J. Polym. Sci., Part A: Polym. Chem.* **2012**, 50, 2889-2897; (b) Y. Wang, J. He, J. Chen, L. Ren, B. Jiang, J. Zhao, *ACS Appl. Mater. Interfaces* **2012**, 4, 2735-2742.

17 N. Pradhan, A. Pal, T. Pal, *Colloids Surf. A* **2002**, 196, 247-257.

18 G. D. Moon, U. Jeong, *Chem. Mater.* **2008**, 20, 3003-3007.

19 J. He, J. Chen, L. Ren, Y. Wang, C. Teng, M. Hong, J. Zhao, B. Jiang, *ACS Appl. Mater. Inter.* **2014**, 6, 2718-2725.